SIMULATION AND DESIGN OF LOW EMITTANCE RF ELECTRON GUN

C. Saisa-ard*, S. Rimjaem, Plasma and Beam Physics (PBP) Research Facility,
Department of Physics and Materials Science, Faculty of Science,
Chiang Mai University, Chiang Mai 50200, Thailand

Abstract

Generation of high-brightness electron beam is one of the most critical issues in development of advanced electron accelerators and light sources. At the Plasma and Beam Physics (PBP) Research Facility, Chiang Mai University, a low emittance RF electron gun is under the development. This RF-gun is planned to be used as an electron source for a future IR/THz FEL facility. An extra resonant cavity is added to the modified design of the existing PBP-CMU RF-gun in order to reduce the transverse sliced emittance. This cell is coupled to the main full-cell via a side-coupling cavity. The electromagnetic field distributions inside the cavities are simulated by using the CST Microwave Studio 2012@. Then, beam dynamic simulations utilizing the program PARMELA are performed. Both RF and beam dynamic simulation results are reported and discussed in this contribution.

INTRODUCTION

The high brightness electron beam is essential in development of the next generation electron accelerators and light sources. The brightness of electron beams depends on the beam peak current and 6-dimensional emittance. This characteristic requires the high quality beams emitting from the electron injector. An electron gun of the linac-based THz radiation source at the Plasma and Beam Physics (PBP) Research Facility, Chiang Mai University, is driven by a 7 MW-klystron at the resonant frequency of 2856 MHz. It consists of 1.6 cell S-band standing-wave structure and a tungsten dispenser thermionic cathode with Os/Ru coating. The present RF-gun design was optimized to produce electron beams with longitudinal distribution suitable for using an alpha magnet as a magnetic bunch compressor. Together with a downstream linac section and related beam transport components, electron beams with the bunch length in order of fermtosecond can be obtained [1]. In order to improve the transverse properties of electron beams, new modified design of the RF-gun is conducted [2]. The previous study results suggest that by adding TM_{010} pillbox cavity next to the main full-cell is able to reduce the sliced emittance and line up the sliced phase spaces [3].

In this work, an extra resonant cavity is added to the PBP-CMU RF electron gun to modify the dynamics of electrons. This extra cell is connected to the end of the full-cell and the RF power is coupled from the full cell to the extra cell via the side coupling cavity. The electromagnetic fields inside the resonant cavities are simulated by using the program CST Microwave Studio (MWS) 2012@ [4]. The dynamics of electrons under the influence of the electromagnetic fields are studied by using a particle tracking program PARMELA [5]. RF parameters of the cavities and beam dynamics study results of electron beams are the main points, which are presented and discussed here.

* chaipattana_s@cmu.ac.th

SIMULATION OF ELECTROMAGNETIC FIELDS

The PBP-CMU RF gun consists of two main cavities, which operates in $\pi/2$ mode for acceleration at the resonant frequency of 2856 MHz. The existing RF-gun has asymmetric shape due to side-coupling cavity opening holes and an RF waveguide input port, which lead to asymmetric beam distribution. By rotating the direction of the side-coupling cavity to vertical direction, the asymmetric feature of electron beams reduced [2]. In this research, an extra cell is added downstream the full cell and it is coupled via a side coupling cavity in vertical direction as shown in Fig. 1 and Fig. 2. The mode of acceleration is kept to be at $\pi/2$ mode and at this mode the resonant frequency of the whole gun is around 2857.3 MHz. The RF parameters for each cell are listed in Table 1.

The electromagnetic field distributions in each mode is solved by using the *Eigenmode Solver* feature in CST MWS. Only boundary conditions at the end of the RF input port and at the end of the extra cell are Dirichelet, otherwise the Neumann boundary conditions is used. The hexahedral mesh is chosen and the total number of mesh cells is 265,650. The amplitude of axial electric field ratio between each cell, which implies to energy gain, can be adjusted by moving tuning rod inside the side coupling cavity. The axial electric field distribution along the beam propagating direction is shown in Fig. 3. The peak field ratio between the cells shown, in Table 2, are adjusted for optimizing electron bunch compression using the alpha magnet, which will be discussed later in other report.

Table 1: RF Parameters of Each Cell at $\pi/2$-mode

RF parameters	half cell	full cell	extra cell
Resonant frequency (MHz)	2866.3	2876.0	2870.0
Shunt impedance (MΩ)	3.45	7.99	5.75
Power (W)	290.8	358.2	318.6
Stored energy (mJ)	0.225	0.378	0.257
R-upon-Q	248	419.34	392.5
Accelerating Voltage (MV)	2.11	2.65	2.63

ISBN 978-3-95450-134-2

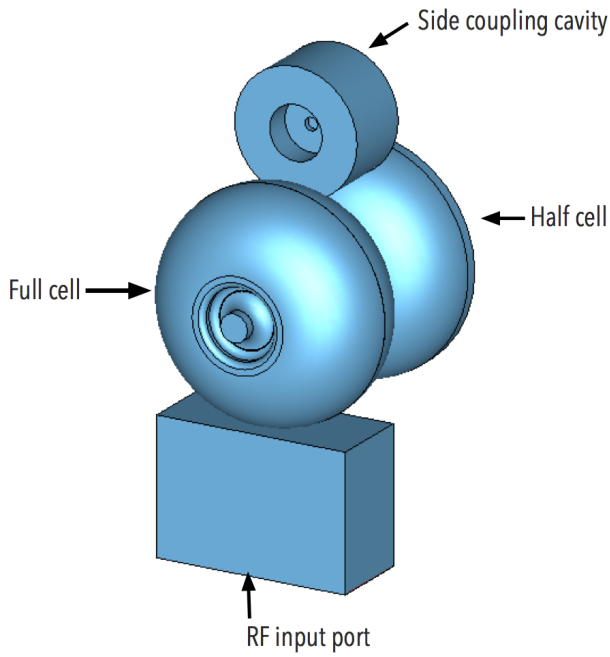

Figure 1: 3D CST MWS model of the thermionic RF-gun at the Plasma and Beam Physics Research Facility, Chiang Mai University.

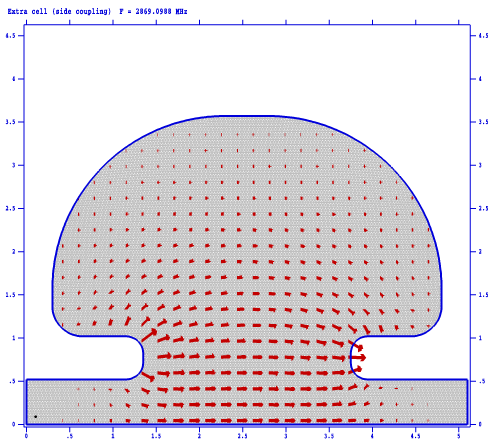

Figure 2: 2D internal geometry and SUPERFISH electric field vectors of the extra-cell (only half of the cell cross-section is shown here).

The axial electric field profile along z-axis can be investigated by varying the tuning rod position inside the side coupling cavity located between the full-cell and the extra-cell. By tuning the length of the tuning rod to be 1.15 mm, the peak field average field ratio between the cells are obtained as listed in Table 2.

BEAM DYNAMICS SIMULATIONS

The electromagnetic field distributions inside the new design RF-gun obtained from the program CST MWS and SUPERFISH [6] are used in the particle-in-cell program PARMELA. In simulations, 100,000 particles are assumed

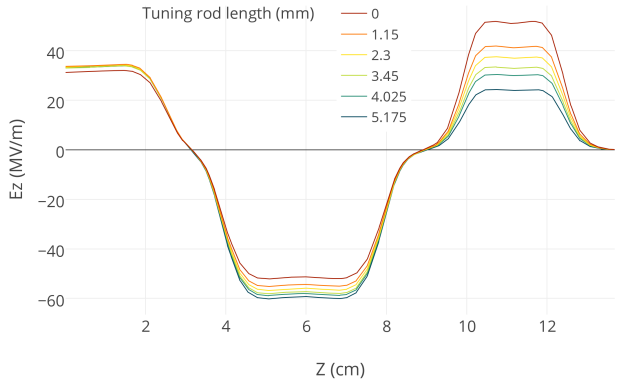

Figure 3: Axial peak electric field along z-direction inside the RF-gun

Table 2: The Peak and Average Field Ratios between Cells

Field ratio	full-cell / half-cell	full cell / extra cell
Peak field ratio	1.52	1.84
Average field ratio	1.59	1.31

to be uniformly emitted from a 3-mm radius thermionic cathode with a total beam current of 2.9 A. An initial energy of the reference particle is set to be 0.10971 eV, corresponding to the cathode temperature of 1,273 K. Energy spreads in both transverse and temporal directions are included in simulations.

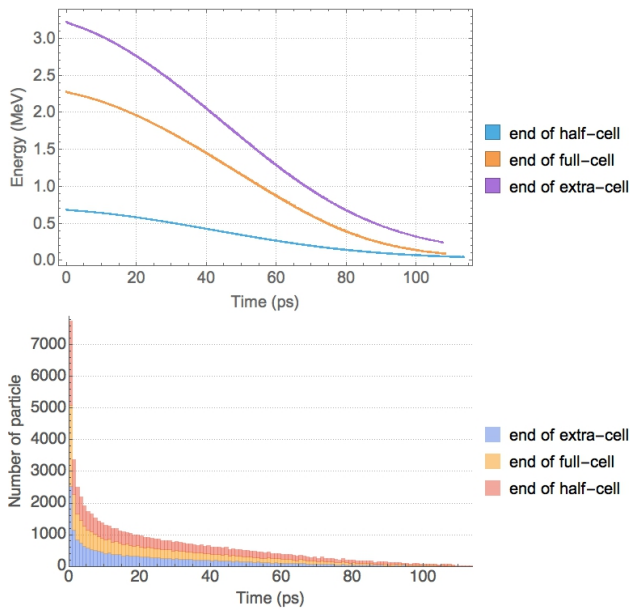

Figure 4: Longitudinal phase spaces and histograms at the ends of the half-cell, full-cell and extra-cell.

Longitudinal phase spaces and their temporal histograms at the ends of half-cell, full-cell and extra cell are shown in Fig. 4. Obviously, the electrons gain kinetic energy while they are moving inside the extra cell. However, it still has the

ISBN 978-3-95450-134-2

linear relation between energy and time at both directions, which is required for the bunch compression by using the alpha magnet.

Simulation results in the transverse direction at the end of the half-cell, full-cell and extra-cell are shown in Figs. 5–7. The vertical phase spaces at the ends of these three cells show asymmetric beam distributions due to non-symmetric magnetic fields in vertical direction (y-axis). This is caused by open holes at the side coupling cavity and the RF input port. The asymmetric beam distribution results in larger transverse beam emittance value and also leads to the off-center of the transverse beam profile.

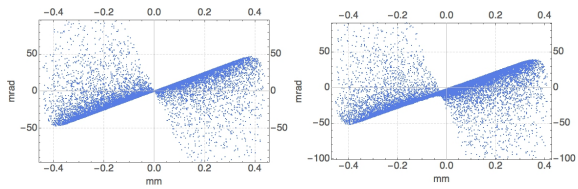

(a) x-axis (b) y-axis

Figure 5: Transverse phase spaces at the end of the half-cell

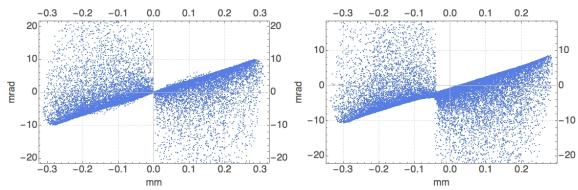

(a) x-axis (b) y-axis

Figure 6: Transverse phase spaces at the end of the full-cell

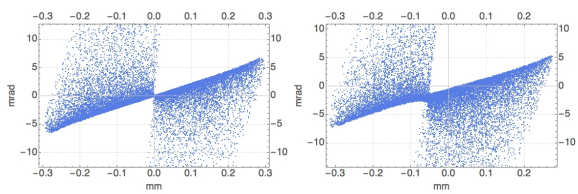

(a) x-axis (b) y-axis

Figure 7: Transverse phase spaces at the end of the extra-cell

The geometrical emittance can be calculated from $\epsilon = \sqrt{< t_i^2 >< (t_i')^2 > - < t_i t_i' >^2}$, where t_i and t_i' are the transverse positions (x or y) and their corresponding transverse momenta, respectively. The normal emittance is then be $\epsilon_n = \beta\gamma\epsilon$. The emittance values at the ends of full-cell and extra-cell are shown in the Table 3.

The sliced phase spaces are studied for the time periods of 0–10 ps and 10–20 ps along the bunch. The results at the ends of full-cell and extra-cell exits are compared in Fig. 8. The two sliced phase spaces at the end of the extra cell are more lined up than ones. The transverse projected emittance value for 90 % of high energetic beam for each time slice along the bunch are plotted in Fig. 9. It is clearly seen that at the tail of electron bunch with the time longer than 45 ps, the transverse projected emittance values at the end of the extra-cell are lower than the beam at the end of the full-cell. The number of electron within 45 ps is approximately 89.5% of the whole bunch.

Table 3: Transverse Emittance Values at The Ends of Full-Cell and Extra-cell

Exit of		100% beam		90% beam	
		x	y	x	y
ϵ (mm mrad)	full-cell	19.3	20.7	5.45	6.85
	extra-cell	9.6	10.4	3.57	4.75
ϵ_n (mm mrad)	full-cell	63.3	68.0	19.4	24.4
	extra-cell	46.5	50.4	18.6	24.8

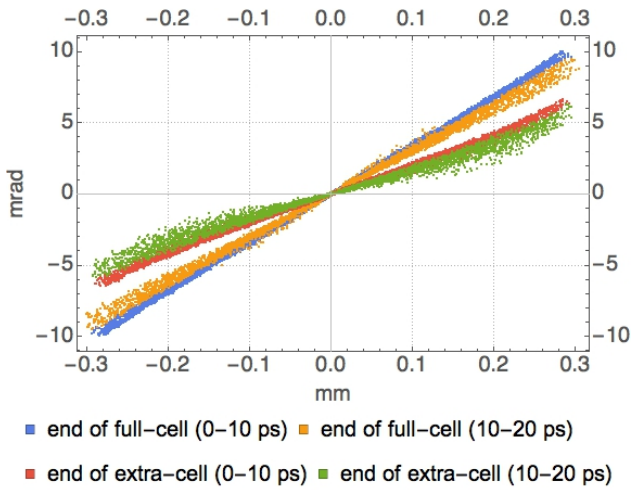

(a) x

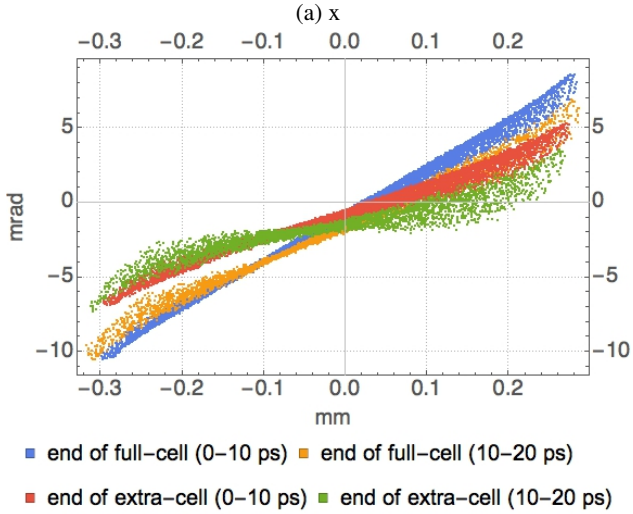

(b) y

Figure 8: The sliced phase spaces for the time periods of 0–10 ps and 10–20 ps along the bunch at the ends of full-cell and extra-cell.

CONCLUSION

Development of a new RF-gun at the PBP-CMU linac facility is on going. The design of the main accelerating

ISBN 978-3-95450-134-2

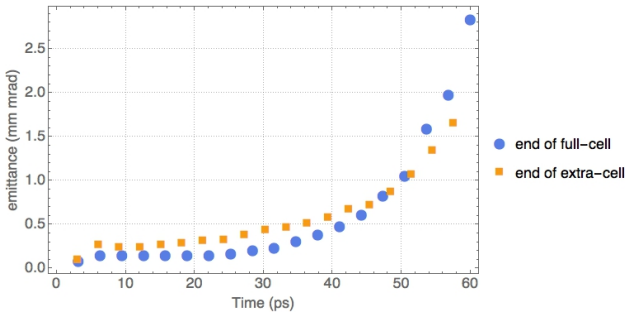

Figure 9: The sliced transverse emittance values, $\epsilon_{xy} = \sqrt{\epsilon_x \epsilon_y}$ along electron bunch at the ends of the full-cell and the extra-cell.

cavities is based on the first PBP-CMU RF-gun with RF-coupling in vertical direction for both RF input port and side-coupling cavity. The extra-cell is added to the full-cell to reduce the transverse emittance in both x and y directions. Although the force due to the electric field inside the extra-cell accelerates the beam, the linear relation between energy-time, which is necessary for bunch compression, still remains. The transverse projected emittance values at the end of the extra-cell are lower than at the end of the full-cell in both x and y directions. The sliced phase spaces within 0-10 ps and 10-20 ps for the x-direction at the extra-cell exit are more lined up than that y-direction.This is due to asymmetric vertical magnetic field distribution which is effected by the opening holes of the side coupling cavity. Furthermore, the sliced emittance values of the particles at the tail of the bunch (> 45 ps) at the end of the extra-cell are lower than that at the end of the full-cell. The trend of the growth of sliced emittance along the whole bunch at the end of extra-cell is also lower.

ACKNOWLEDGMENT

The authors would like to acknowledge the support from the CMU Junior Research Fellowship Program and the Department of Physics and Materials Science, Faculty of Science, Chiang Mai University.

REFERENCES

[1] C.Thongbai et al., Nucl. Instrum. Meth. A **587**, p. 130 (2008).

[2] S. Rimjaem et al., Nucl. Instrum. Meth. A **736**, p. 10 (2014).

[3] K. Kusoljariyakul et al., Nucl. Instrum. Meth. A **645**, p. 191 (2011).

[4] Microwave Studio, Computer Simulation Technology, Darmstadt, Germany. `http://www.cst.com`

[5] L.M. Young et al., PARMELA, Los Alamos National Laboratory Technical Note LA-UR-96-1835 (2002).

[6] K. Halbach et al., Part.Accel. **7**, p. 213 (1976).

ISBN 978-3-95450-134-2